Complexation of Ammonia Boranes with Al³⁺

Iurii Dovgaliuk,*[,†,‡] Kasper T. Møller,[†,§] Koen Robeyns,[†] Véronique Louppe,[†] Torben R. Jensen,[§] and Yaroslav Filinchuk*[,†]

†Institute of Condensed Matter and Nanosciences, Université catholique de Louvain, place L. Pasteur 1, B-1348 Louvain-la-Neuve, Belgium

‡Swiss−Norwegian Beamlines at the European Synchrotron Radiation Facility, 71 avenue des Martyrs, F-38000 Grenoble, France

§Interdisciplinary Nanoscience Center and Department of Chemistry, University of Aarhus, Langelandsgade 140, DK-8000 Aarhus C, Denmark

ⓢ *Supporting Information*

ABSTRACT: Ammonia borane, NH_3BH_3 (AB), is very attractive for hydrogen storage; however, it dehydrogenates exothermally, producing a mixture of polymeric products with limited potential for direct rehydrogenation. Recently, it was shown that AB complexed with Al^{3+} in $Al(BH_4)_3 \cdot AB$ endothermically dehydrogenates to a single product identified as $Al(BH_4)_3 \cdot NHBH$, with the potential for direct rehydrogenation of AB. Here we explore the reactivity of AB-derived RNH_2BH_3 (R = $-CH_3$, $-CH_2-$) with AlX_3 salts (X = BH_4^-, Cl^-), aiming to extend the series to different anions and to enlarge the stability window for $Al(BH_4)_3 \cdot NRBH$. Three novel complexes were identified: $Al(BH_4)_3 \cdot CH_3NH_2BH_3$ having a molecular structure similar to that of $Al(BH_4)_3 \cdot AB$ but different dehydrogenation properties, as well as $[Al(CH_3NH_2BH_3)_2Cl_2][AlCl_4]$ and $[Al(NH_2CH_2CH_2NH_2)(BH_4)_2][Al(BH_4)_4]$, rare examples of Al^{3+} making part of the cations and anions simultaneously. The latter compounds are of interest in the design of novel electrolytes for Al-based batteries. The coordination of two ABs to a single Al atom opens a route to materials with higher hydrogen content.
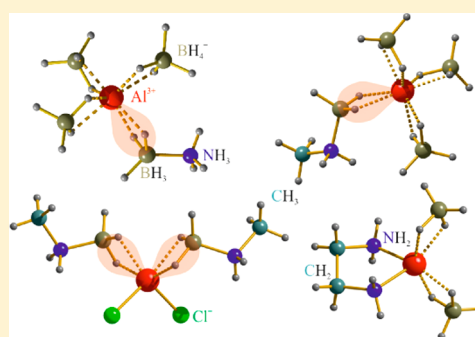
INTRODUCTION

Solid-state hydrogen storage is one of the main challenges for the worldwide use of this environmentally benign fuel. In recent years, metal borohydrides $[M(BH_4)_n]$[1,2] and M−B−N−H systems[3,4] of metal amidoboranes (MABs), amine metal borohydrides, and complexes with ammonia borane, NH_3BH_3 (AB), have been intensively explored as the most attractive materials for potential solid-state hydrogen storage.[5]

AB is a promising hydrogen storage candidate because of its high hydrogen content (~19.6 wt %) and acceptable stability upon transportation and storage.[6,7] Pristine AB undergoes a stepwise decomposition, with 6.5 wt % hydrogen released below 112 °C and 14.5 wt % near 200 °C. However, both steps are accompanied by the release of undesirable borazine and the formation of stable polyaminoborane, $(NH_2BH_2)_n$. A complicated mixture of the dehydrogenation products can hardly be regenerated in one step, unless a mixture of hydrazine/ammonia is used.[8,9] However, recently investigated metal borohydride−AB complexes, $M(BH_4)_n(AB)_m$ (n = 1, m = 1 or 2 for M = Li^+; n = m = 2 for M = Ca^{2+} and Mg^{2+}), showed more facile hydrogen desorption with less ammonia evolution compared to pure AB and MABs.[10−13] Moreover, our recent investigation of the $Al(BH_4)_3 \cdot AB$ complex established high-purity hydrogen release at moderate temperature (70 °C), according to the reaction[14]

$$Al(BH_4)_3 \cdot NH_3BH_3 \rightarrow Al(BH_4)_3 \cdot NHBH + 2H_2 \qquad (1)$$
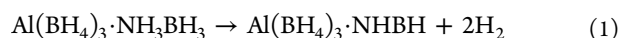
$Al(BH_4)_3 \cdot AB$ is also encouraging in terms of a possible direct rehydrogenation of AB,[14,15] which is typically regenerated via multistep chemical cycles.[16] The striking property of $Al(BH_4)_3 \cdot AB$ is endothermic dehydrogenation in the first decomposition step [reaction (1); ΔH_{dec} = 39 kJ/mol, including melting], compared to the exothermic one for AB (ΔH_{dec} = −22 kJ/mol on the first decomposition step, including melting).[6] Endothermic dehydrogenation enables this system to be potentially reversible upon direct rehydrogenation, and the absence of complicated mixtures after dehydrogenation may allow for a viable chemical recycling of AB.

Substitution of AB on the nitrogen side is an interesting way to prevent the second decomposition step of $Al(BH_4)_3 \cdot NH_3BH_3$, while retaining the endothermic character of the reaction (1). More precisely, the aim is to extend the stability range of $Al(BH_4)_3 \cdot NHBH$, which decomposes just above 90 °C, releasing heavier gas molecules and thus losing the potential for reversibility. We have chosen the lightest substituted AB, namely, methylamine borane, $CH_3NH_2BH_3$ (MeAB), and ethylenediamine bis(borane), $(CH_2NH_2BH_3)_2$

(EDBB). These AB derivatives can be easily obtained from commercially available chemicals and have previously been investigated as potential hydrogen carriers. However, the neat materials have several disadvantages for hydrogen storage. In particular, MeAB exhibits a high degree of volatility upon thermal treatment,[17] and EDBB has a higher thermal stability compared to its parent counterparts, AB and MeAB.[18,19] Moreover, in contrast to the numerous investigations on $M(BH_4)_n(AB)_m$, there is no information about MeAB and EDBB analogues with borohydrides to date.

The second improvement of the $Al(BH_4)_3 \cdot AB$ model system can be achieved by substitution of the pyrophoric $Al(BH_4)_3$ by $AlCl_3$. Exchange of the formally inert anion, however, should alter the electronic properties of the Al cation, as well as destabilize the structure containing a network of dihydrogen bonds.[14] In this work, the expected $AlX_3 \cdot BH_3NH_2R$ (X = BH_4^-, Cl^-; R = −H, −CH$_3$, −CH$_2$−) complexes were explored, and the products were characterized structurally. Three new compounds were obtained, with only one of them, $Al(BH_4)_3 \cdot MeAB$, adopting a molecular structure analogous to that of $Al(BH_4)_3 \cdot AB$. The other compounds, $[Al(MeAB)_2Cl_2]$-$[AlCl_4]$ and $[Al(en)(BH_4)_2][Al(BH_4)_4]$, contain Al^{3+} in their cations and anions simultaneously; the ethylenediamine (en) complex forms via borane splitting from EDBB. Surprisingly, the reaction of $AlCl_3$ with AB does not lead to the AB complex but yields NH_4AlCl_4.[20] Overall, $Al(BH_4)_3 \cdot MeAB$ is the most similar to $Al(BH_4)_3 \cdot AB$ by composition and molecular structure. Thus, it has been studied in detail by in situ synchrotron powder X-ray diffraction (PXRD), thermogravimetric analysis and differential scanning calorimetry coupled with mass spectrometry (TGA/DSC/MS), temperature-programmed photographic analysis (TPPA), and volumetric methods in order to compare its hydrogen storage properties with those of $Al(BH_4)_3 \cdot AB$.

We show that the proposed modifications apply to the model system, despite only in part allowing for the rational design of the AB series templated on Al^{3+}. Interestingly, two AB molecules can be coordinated by a single Al^{3+} ion, potentially bringing the gravimetric capacity of these systems closer to practical.

■ RESULTS AND DISCUSSION

Below we describe the formation and structures of the new compounds, followed by a detailed characterization of the stability and dehydrogenation for a new molecular analogue of the model system $Al(BH_4)_3 \cdot MeAB$.

Formation of Al Complexes with ABs. The interaction of AlX_3 (X = BH_4^- and Cl^-) with light amine boranes BH_3NH_2R (R = −H, −CH$_3$, −CH$_2$−) results in three new AB-based complexes (see the Experimental Section and Table 1). Single-crystal X-ray diffraction and PXRD reveal the formation of a single-phase $Al(BH_4)_3 \cdot MeAB$ having a molecular structure identical with that of the model compound $Al(BH_4)_3 \cdot AB$. Replacing the borohydride group by chloride, with the use of pristine AB, leads to the formation of crystalline NH_4AlCl_4 (Figure S1).[20] NMR spectroscopy studies of the reaction product, described in the Supporting Information, reveal no NH_3BH_3, BH_4^-, or aminodiborane $[BH_3NH_2BH_3]^-$ anions but the presence of $[NH_3BH_2NH_3]^+$.[21] Double substitution both on the N side of AB and on the anion site reveals a complex containing two MeAB coordinated to a single Al^{3+}. The single-crystal structure gives a composition $[Al(MeAB)_2Cl_2][AlCl_4]$, where tetrachloroalanate serves as a counterion.

The use of substituted AB in the form of a dimer, EDBB, leads to the slow formation of an en complex with the composition $[Al(en)(BH_4)_2][Al(BH_4)_4]$. This product suggests the elimination of diborane B_2H_6 from EDBB upon formation of the stable chelate complex with Al. Very low concentrations of en forming in situ upon complexation with $Al(BH_4)_3$ result in a complex with a very high $Al(BH_4)_3$-to-n(en) ratio of 1:2. en-rich compounds $Al(BH_4)_3 \cdot n$en ($1 \leq n \leq 4$) were obtained by a direct reaction between the components,[22,23] but the $n = 1:2$ ratio was not achievable by this method. The B−N bond splitting places the chemistry of this system far away from that of $Al(BH_4)_3 \cdot AB$. Most likely, these Al-EDBB-based systems are less stable and not suitable for reversible hydrogen storage. EDBB does not yield any products with $AlCl_3$ at ambient conditions.

Molecular and Crystal Structures of $Al(BH_4)_3 \cdot MeAB$. $Al(BH_4)_3 \cdot MeAB$ crystallizes in the triclinic space group $P\bar{1}$ [$a = 6.2764(3)$ Å, $b = 7.9566(5)$ Å, $c = 10.3058(8)$ Å, $\alpha = 70.28(1)°$, $\beta = 74.74(1)°$, and $\gamma = 86.04(1)°$]. It adopts a molecular structure and resembles the heteroleptic complex of $Al(BH_4)_3 \cdot AB$;[14] see the comparison in Figure 1.
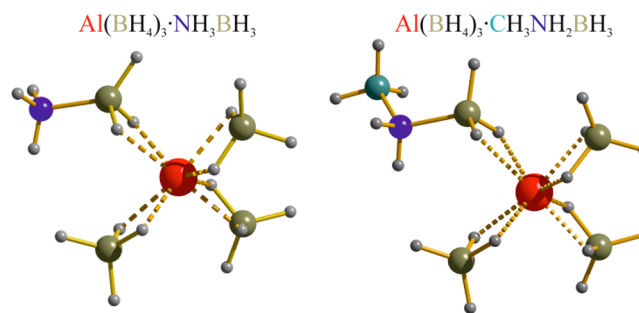

Figure 1. Isolated $Al(BH_4)_3 \cdot AB$ and $Al(BH_4)_3 \cdot MeAB$ complexes, where the Al^{3+} cation coordinates three BH_4^- anions and one AB or MeAB molecule. Color code: Al, red; B, olive; N, blue; C, teal; H, gray.

Al atoms coordinate three BH_4^- anions and one MeAB molecule, forming a mononuclear complex. The Al^{3+} cation is linked via BH_2 edges and hence adopts a distorted tetrahedral coordination made up of borohydride groups, while the AlH_8 polyhedron has the shape of a snub disphenoid, similar to Al in $Al(BH_4)_3 \cdot AB$ or Mg in $Mg(BH_4)_2$.[14,24,25] The Al···B distances with the BH_4^- ions are in the narrow range of 2.22−2.24 Å, similar to 2.21−2.23 Å in the two $Al(BH_4)_3 \cdot NH_3BH_3$ polymorphs. This distance is nearly identical with the Al···B distances of 2.22−2.26 Å in $M[Al(BH_4)_4]$ (M = Li$^+$, Na$^+$, K$^+$, NH_4^+, Rb$^+$, Cs$^+$) and $[Ph_3MeP][Al(BH_4)_4]$, where the Al^{3+} cation is also coordinated to eight H atoms.[31−33] The interatomic Al···B contact involving the MeAB's BH_3 group is slightly longer (2.34 Å) than the distances to the BH_4^- anions, fully consistent with the elongation in $Al(BH_4)_3 \cdot AB$ (2.31 Å). However, they remain much shorter than the metal−boron distances in metal borohydride−AB complexes, namely, 2.63−2.92 Å in $(LiBH_4)_2 \cdot AB$, $LiBH_4 \cdot AB$, and $Ca(BH_4)_2 \cdot (AB)_2$.[10,11] Al−H bond distances vary accordingly: for the BH_4^- groups, they range from 1.76(2) to 1.80(2) Å, similar to those in Al-based complex hydrides,[31−33] and vary from 1.89(1) to 1.96(1) Å, where the AB's −BH_3 group is involved.[14]

The molecules of $Al(BH_4)_3 \cdot MeAB$ are linked via simple and bifurcated $N−H^{\delta+} \cdots H^{\delta-}−B$ dihydrogen bonds with H···H

distances of 2.10−2.42 Å and H···H−N angles of 130−160°
(Figure 2). These values are slightly below the sum of the van
der Waals distances of 2.4 Å and are in agreement with the
directionality criterion accepted for the dihydrogen bonds.[26]
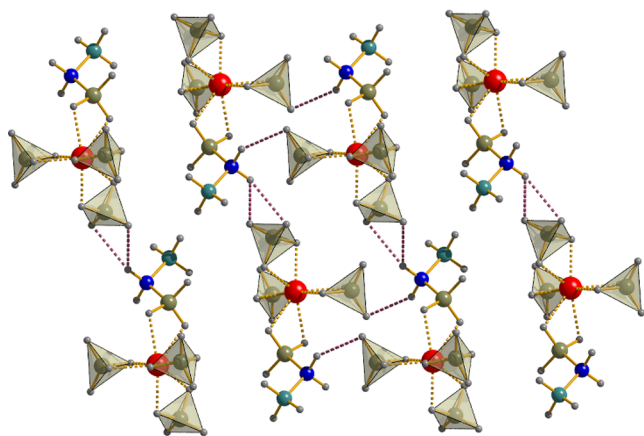
Figure 2. $Al(BH_4)_3 \cdot MeAB$ molecules linked via dihydrogen bonds, depicted by violet dashed lines.

Crystal Structures of $[Al(MeAB)_2Cl_2][AlCl_4]$ and $[Al(en)(BH_4)_2][Al(BH_4)_4]$.

According to the CCDC[27] and ICSD databases,[28] $[AlCl_2L_2]^+$ (L-ligand) complexes are fairly rare (two examples are known to date),[29,30] and the formation of an autoionized borohydride complex (containing Al in both cationic and anionic forms) was found for the first time.

$[Al(MeAB)_2Cl_2][AlCl_4]$ crystallizes in the orthorhombic crystal system, space group $Pbca$ [a = 12.5826(5) Å, b = 12.6510(5) Å, and c = 20.4039(8) Å]. The $[Al(MeAB)_2Cl_2]^+$ cation adopts a slightly distorted tetrahedral coordination with ∠B···Al···B of 104.1(2)° and ∠Cl···Al···Cl of 108.5(6)°, comparable to ∠Cl···Al···Cl 107.9(7)−112.1(7)° in the $[AlCl_4]^-$ anion (Figure 3). The 96.7(1)−125.3(1)° range of
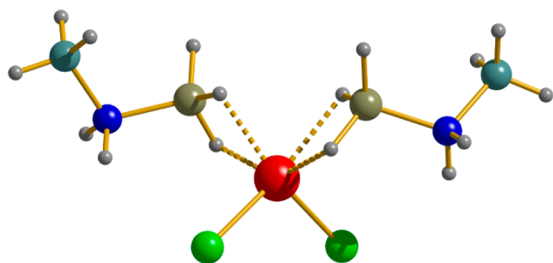
Figure 3. Representation of the $[Al(MeAB)_2Cl_2]^+$ cation in $[Al(MeAB)_2Cl_2][AlCl_4]$. Color code: Al, red; B, olive; Cl, green; N, blue; C, teal; H, gray.

the Cl···Al···B angles is closer to the B···Al···B angle range in homoleptic $M[Al(BH_4)_4]$ (M = Li^+, Na^+, K^+, NH_4^+, Rb^+, Cs^+) and $[Ph_3MeP][Al(BH_4)_4]$[31−33] than to the nearly ideal tetrahedral coordination in the heteroleptic complex anion $[Al(BH_4)_2Cl_2]^-$.[34] Al···Cl distances in the $[Al(MeAB)_2Cl_2]^+$ cation of 2.11(1) and 2.14(1) Å are in good agreement with 2.1−2.3 Å in other cationic complexes of Al.[35] The MeAB ligand coordinates to Al via bridging H atoms of the BH_3 groups with Al···B and Al−H distances of 2.24(5)−2.26(4) and 1.8(2)−1.9(2) Å, respectively, much like those in the MeAB complex with $Al(BH_4)_3$ (see above). The C−N and B−

N distances of 1.48(5) and 1.57(5) Å are nearly the same as those in the noncomplexed MeAB.[17,36]

$[Al(en)(BH_4)_2][Al(BH_4)_4]$ crystallizes in the monoclinic crystal system, space group $P2_1/c$ [a = 8.4168(5) Å, b = 12.0021(7) Å, c = 16.2933(12) Å, and β = 101.89(1)°]. Among the previously reported complexes of $Al(BH_4)_3$ with en, several compositions of $Al(BH_4)_3 \cdot n(en)$ ($1 \leq n \leq 4$) have been proposed;[22] however, the only crystal structure characterized to date is that for $[Al(en)_3][BH_4]_3 \cdot (en)$.[23]

Both complex ions in $[Al(en)(BH_4)_2][Al(BH_4)_4]$ adopt distorted tetrahedral coordination for Al atoms with respect to B and N atoms (Figure 4). The ∠N···Al···N of 86.5(2)° is
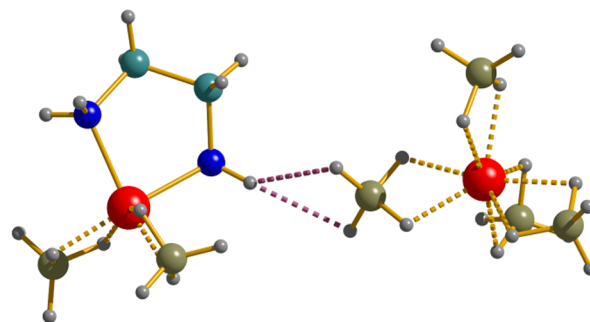

Figure 4. $[Al(en)(BH_4)_2]^+$ cation and $[Al(BH_4)_4]^-$ anion connected via bifurcated dihydrogen bonds (violet dashed lines). Color code: Al, red; B, olive; N, blue; C, teal; H, gray.

similar to those of other known bidentate chelates of Al.[35] The B···Al···B angle of 118.1(3)° in the cation is close to tetrahedral, while the angles around Al in the $[Al(BH_4)_4]^-$ anion range from 98.9(3) to 135.4(3)°, typical for a slightly flattened tetrahedron. This geometry is identical in aluminum borohydrides of alkali metals $M[Al(BH_4)_4]$ (M = Li^+, Na^+, K^+, NH_4^+, Rb^+, Cs^+) and in $[Ph_3MeP][Al(BH_4)_4]$.[31−33] $[Al(en)(BH_4)_2]^+$ contains a chelate cycle involving en and two BH_4^- groups coordinated via BH_2 edges (Figure 4). The Al···B distances of 2.16(7) and 2.17(8) Å in the cation are slightly shorter than 2.23(8)−2.27(8) Å in the $[Al(BH_4)_4]^-$ anion.[31−33] The Al···N distances of 1.95(4) and 1.96(4) Å are typical (1.9−2.0 Å) for other Al-containing cations.[35] The Al···H distances of 1.72(4)−1.77(5) Å in the cation and 1.79(4)−1.89(4) Å in the anion are correlated with the Al···B distances. The structure is stabilized by simple and bifurcated dihydrogen $N-H^{\delta+} \cdots H^{\delta-}-B$ bonds with H···H distances of 2.02−2.22 Å and H···H−N angles of 140−160°.

Analysis of $Al(BH_4)_3 \cdot MeAB$ Thermal Decomposition.

Variable-temperature synchrotron radiation PXRD on $Al(BH_4)_3 \cdot MeAB$ shows that $Al(BH_4)_3 \cdot MeAB$ is a single phase that melts around 50 °C (Figure 5). According to TGA/DSC (Figure 6), the forming liquid decomposes in three well-defined steps, and no other crystalline products were observed upon heating up to 80 °C (Figure 5). $Al(BH_4)_3 \cdot MeAB$ was investigated using TGA/DSC/MS, volumetric analysis, and TPPA (Figures 6−9). The general conclusion is that its decomposition is complicated and does not follow the hydrogen release mechanism of the parent $Al(BH_4)_3 \cdot AB$. In particular, the TGA/DSC/MS data suggest three distinct steps, while two decomposition steps have been observed for $Al(BH_4)_3 \cdot AB$.
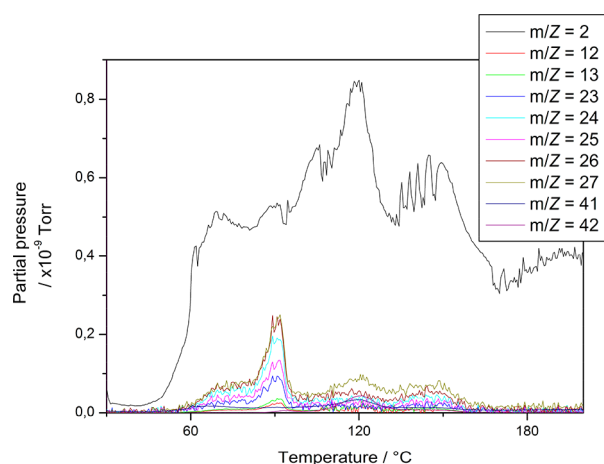
The first decomposition step initiates already at T = 50 °C and corresponds to an endothermic peak at 57 °C, which is in
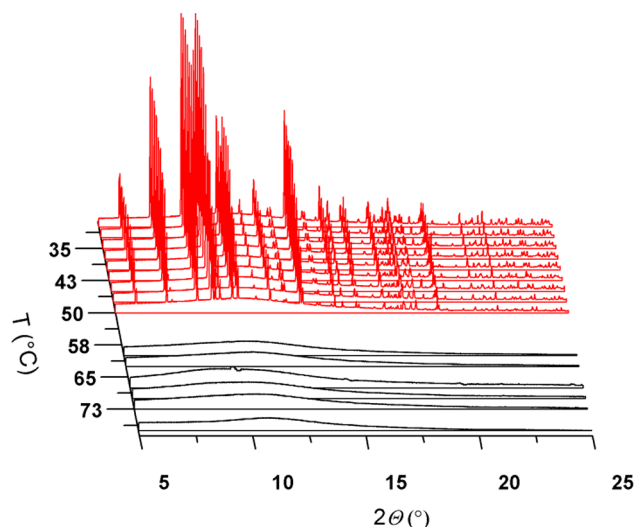
Figure 5. Temperature evolution of in situ synchrotron PXRD patterns for Al(BH₄)₃·MeAB.
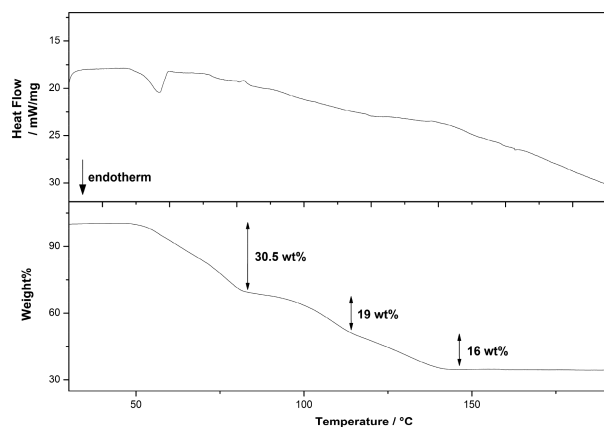

Figure 6. DSC (upper) and TGA (lower) data for Al(BH₄)₃·MeAB decomposition measured from room temperature to 200 °C (ramp rate = 1 K/min).

**Figure 7.** MS data for Al(BH₄)₃·MeAB decomposition measured from room temperature to 200 °C (ramp rate 1 = °C/min).

good agreement with the melting point of the crystalline sample observed by in situ PXRD and is close to the melting point of pure MeAB (58−59 °C).[37] Thus, the evolved gases during thermal treatment could come from intermolecular
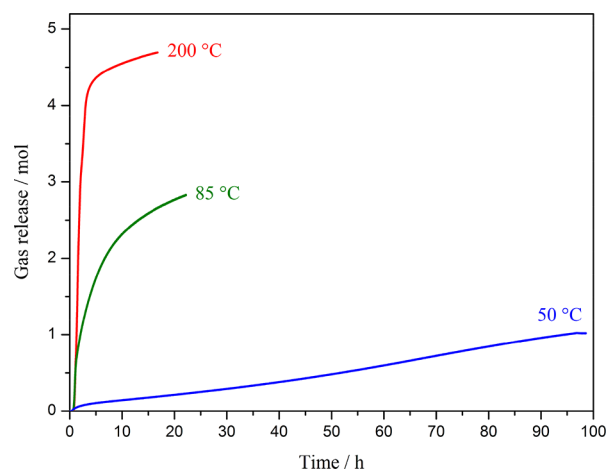

Figure 8. Volumetric measurements on Al(BH₄)₃·MeAB samples heated from room temperature to 50 °C (blue), 85 °C (green), and 200 °C (red) ($\Delta T / \Delta t$ = 1 °C/min), revealing releases of ∼1, ∼3, and ∼5 mol of gas per mole of the complex, respectively.
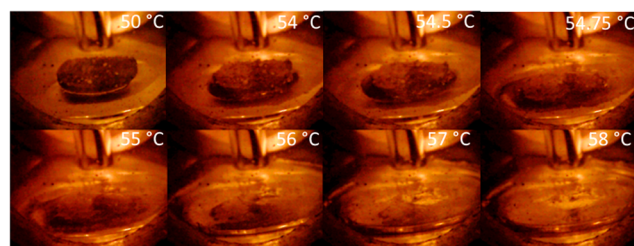

Figure 9. TPPA of Al(BH₄)₃·MeAB heated from room temperature to 80 °C (ramp rate = 1 °C/min) showing fast degradation of the sample in a narrow temperature range.

reactions between Al(BH₄)₃ and MeAB or thermal decomposition of either MeAB or Al(BH₄)₃ or both. The mass loss of ∼30.5 wt % observed by TGA on the first step corresponds to ∼1 mol of the released gas products seen by the volumetric measurements at 50 °C (Figures 6 and 8). This suggests an equimolar release of volatile product(s), such as methylamine (CH₃NH₂; expected mass loss = 26.3 wt %), HCN (22.8 wt %), and/or other species, such as diborane B₂H₆ (23.4 wt %). It is practically impossible to distinguish in the laboratory MS data the m/z values for HCN and B₂H₆ because of the resolution limitations (e.g., at 26 and 27).[38] However, the investigated MS range of m/z 1−50 must show a hydrogen release (m/z 2) and B₂H₆ (or HCN) evolution (in the range of m/z 23−27).[39] Hydrogen may originate from the decomposition of diborane in the transfer line to MS. The strongest peaks characteristic for CH₃NH₂ (m/z 28, 30, and 31) have not been observed, suggesting that MeAB or its organic parts are not leaving the complex. We are not certain about the thermolysis products, but the observed data can be rationalized by reaction (2), giving ∼24 wt % volatile products.

$$Al(BH_4)_3 \cdot CH_3NH_2BH_3$$
$$\rightarrow [HAl(BH_4)_2] \cdot CH_3NH_2 + B_2H_6 \qquad (2)$$
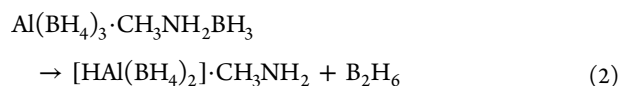
The second decomposition step takes place between 82 and 115 °C with a mass loss of another 19 wt % and a weak exothermic peak at $T \sim 82$ °C. It is initiating a sudden increase of B₂H₆ desorption along with signals at m/z 12 and 13, indicative for HCN. Reaction (2), followed by a release of

HCN, can reach 50.4 wt % compared to the observed 49.5 wt % loss and the release of 4 mol of gas. Despite the fact that our volumetric experiment reached only 3 mol of the released gas at 85 °C, this value was limited by kinetics (Figure 8). The overall reaction for the two first decomposition steps can be presented as

$$2Al(BH_4)_3 \cdot CH_3NH_2BH_3$$
$$\rightarrow [HAl(BH_4)_2]_2 + 2B_2H_6 + 2HCN + 4H_2 \quad (3)$$
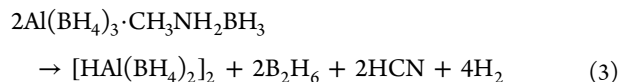
Finally, the third decomposition step occurs in the temperature range of 115−145 °C with yet another loss of 16 wt %. Unfortunately, instrumental artifacts make the interpretation of the DSC signal impossible in this range. MS registered a slight increase at m/z 41 and 42 at ~120 °C. These values have previously been reported for the decomposition of $Al(BH_4)_3$ and/or its derivative $[HAl(BH_4)_2]_2$.[40,41]

Our initial TGA/MS experiment at a high ramp rate has shown a sudden evolution of gases from $Al(BH_4)_3 \cdot MeAB$, so that the lid on the Al_2O_3 crucible was blown off at $T \sim 60$ °C, while TGA also indicated a sudden event. To investigate this behavior further, TPPA was performed (Figure 9). The sample pellet begins to degrade at 50 °C in agreement with the observations in TGA/DSC/MS and the in situ PXRD. The pellet breaks in the narrow temperature range of 54−56 °C and nearly vanishes, leaving only a very small amount of powder in the bottom of the glass tube at 58 °C. This confirms that decomposition indeed occurs rapidly.

We conclude that methyl substitution on the N side of AB leads to decomposition of $Al(BH_4)_3$, coming as the first step of the $Al(BH_4)_3 \cdot MeAB$ thermolysis, instead of AB dehydrogenation in the model $Al(BH_4)_3 \cdot AB$. It is thus necessary to focus on other Al salts capable of coordinating to the modified AB.

Thermal decomposition of these complexes may be better understood considering how strong the bonding interactions are. The bidentate coordination of the metal atom from two B−H bonds, $M \cdots H_2B$ (η^2), is known to be the most stable geometry in metal borohydrides, where the BH_4 ligand bears a negative charge.[5] In the case of neutral substituted AB molecules, the bond energy is expected to be lower but still significant in our case, considering the high charge and polarizing power of the Al^{3+} cation. The $Al^{3+} \cdots H_2B$ bonding energy is likely similar to that in σ-borane complexes,[42] estimated at 20 kcal/mol,[43] i.e., significantly higher than 4−6 kcal/mol per N−H $\cdots$ H−B interaction[44] but lower than the interaction energy of the coordinate covalent B−N bond.[45]

CONCLUSION

The present study shows that $Al(BH_4)_3 \cdot AB$ can be used as a model system in the endeavor of designing hydrogen storage materials based on ABs. Indeed, substitutions on the N side of AB and on the anion site of AlX_3 lead to stable complexes: $Al(BH_4)_3 \cdot MeAB$ and autoionized $[Al(MeAB)_2Cl_2][AlCl_4]$ and $[Al(en)(BH_4)_2][Al(BH_4)_4]$. Coordination of two ABs to a single Al in the $[Al(MeAB)_2Cl_2]^+$ cation opens a route to materials with higher hydrogen content.

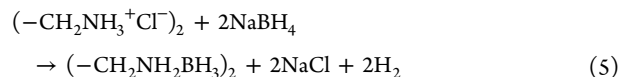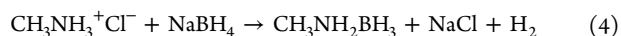Despite the structural and compositional similarities of $Al(BH_4)_3 \cdot AB$ and $Al(BH_4)_3 \cdot MeAB$, their hydrogen storage properties are very different. In contrast to $Al(BH_4)_3 \cdot AB$ releasing H_2 from the coordinated AB, $Al(BH_4)_3 \cdot MeAB$ reveals the decomposition of $Al(BH_4)_3$ with a loss of B_2H_6. This makes clear the need to exchange the borohydride anion for less reactive counterions, as we attempted with Cl^-. Indeed, the idea of the double substitution on $Al(BH_4)_3 \cdot AB$ seems to be the right strategy, and the yield and purity of the other complexes reported here should be improved in order to investigate their hydrogen storage properties.

Compact energy storage systems based on Al are of great interest not just for hydrogen storage.[42] With respect to its potential battery applications, Al has almost 4 times higher volumetric energy density than Li. The autoionized Al complexes $[Al(MeAB)_2Cl_2][AlCl_4]$ and $[Al(en)(BH_4)_2][Al(BH_4)_4]$ fall into the family of potential novel electrolytes for Al^{3+}-based batteries, currently using mainly $[AlCl_4]^-$ molten salts and ionic liquids.[46] The latter $Al(BH_4)_3 \cdot \frac{1}{2}(en)$ complex is a close analogue of $Mg(BH_4)_2 \cdot (en)$, one of the best Mg^{2+}-ion conductors.[47]

EXPERIMENTAL SECTION

Synthesis of MeAB and EDBB. The powders of MeAB and EDBB were obtained according to the simplified procedures described in the literature.[15,48] These syntheses were performed using commercially available methylamine hydrochloride and ethylenediamine dihydrochloride (both from Sigma-Aldrich, 98%) and $NaBH_4$ (Alfa Aesar, 97%). A total of 37 mmol of $NaBH_4$ and stoichiometric amounts of methylamine hydrochloride or ethylenediamine dihydrochloride according to reactions (4) and (5) have been dissolved in 125 mL of tetrahydrofuran and were stirred for ~24 h at room temperature.

$$CH_3NH_3^+Cl^- + NaBH_4 \rightarrow CH_3NH_2BH_3 + NaCl + H_2 \quad (4)$$

$$(-CH_2NH_3^+Cl^-)_2 + 2NaBH_4$$
$$\rightarrow (-CH_2NH_2BH_3)_2 + 2NaCl + 2H_2 \quad (5)$$

The obtained mixtures were filtered in air, and the solvent was removed from the filtrates with a rotary evaporator. Hexane was added to the resulting viscous liquids to precipitate crystals of MeAB or EDBB. PXRD confirmed the purity of the products (Figures S2 and S3).

Interaction of $AlCl_3$ with NH_3BH_3. $AlCl_3$ (Sigma-Aldrich, 95%) and NH_3BH_3 (Sigma-Aldrich, 97%) were loaded under Ar in a 1:1 molar ratio into a ball milling jar and ground for 1 h, yielding a sticky product, where the starting $AlCl_3$ is the only crystalline phase detected by diffraction at room temperature. The same behavior was observed with hand grinding of the mixture in an agate mortar.

Additionally, solvent-mediated synthesis was performed in Et_2O. A total of 2.63 mmol of $AlCl_3$ was dissolved in 6 mL of Et_2O and 2.59 mmol of NH_3BH_3 in 20 mL of Et_2O, and the two solutions were mixed and stirred for 60 h at room temperature. The solution was filtered, and the filtrate was placed on a Schlenk line to dry. The sticky product could not be crystallized with n-hexane; thus, high vacuum (10^{-5} mbar) was applied, resulting in a slurry. Its PXRD analysis reveals the formation of NH_4AlCl_4 and an unknown monoclinic phase with nearly the same unit cell volume (Figure S1). Heating of this mixture results in the substantial growth of NH_4AlCl_4 diffraction peaks at around 60 °C (Figures S4 and S5), suggesting that it can be another polymorph of NH_4AlCl_4. We are not certain about the chemical reaction between $AlCl_3$ and AB, stating only the appearance of NH_4AlCl_4 from X-ray diffraction and the presence of $[NH_3BH_2NH_3]^+$ from solution NMR spectroscopy.

Interaction of $AlCl_3$ and MeAB. Stoichiometric amounts of MeAB and $AlCl_3$ were mixed in an Ar atmosphere. The mixture readily melts/reacts at room temperature, giving a slurry that can be crystallized at −35 °C. Single-crystal X-ray diffraction reveals the formation of $[Al(MeAB)_2Cl_2][AlCl_4]$, according to the reaction

$$2AlCl_3 + 2CH_3NH_2BH_3 \rightarrow [Al(CH_3NH_2BH_3)_2Cl_2][AlCl_4] \quad (6)$$
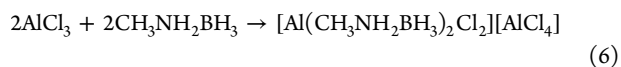
However, this is not the only crystalline phase observed by PXRD, and we were not able to characterize in detail the other crystalline product(s) (Figure S6). Solution NMR spectroscopy shows that ^{1}H-decoupled ^{27}Al NMR spectra are identical with the coupled ones, meaning there is no H directly next to Al, implying that the $[AlCl_2(BH_3NH_2Me)_2]$ cation is not stable in solution. The $AlCl_4$ anion is present as a peak at 70 ppm. A TGA/DSC/MS study shows a significant weight loss starting from ~120 °C, producing CH_3Cl (Figures S7−S9). Decomposed products obtained at 300 °C were not soluble in dimethyl sulfoxide and benzene.

Interaction of AlCl$_3$ with (CH$_2$NH$_2$BH$_3$)$_2$. In contrast to the spontaneous reaction of AlCl$_3$ with MeAB, the same attempt with $(CH_2NH_2BH_3)_2$ in a 1:1 or 2:1 molar ratio yielded no new products at room temperature, as well as upon heating to 70 and 85 °C, respectively, resulting in only melts.

Synthesis of Al(BH$_4$)$_3$·MeAB. *Caution! All of the manipulations with highly pyrophoric Al(BH$_4$)$_3$ must be performed in a glovebox with an inert dry atmosphere!* The reaction conditions to obtain Al(BH$_4$)$_3$·MeAB are similar to those used for the preparation of Al(BH$_4$)$_3$·NH$_3$BH$_3$.[14] The amounts of reagents can be safely scaled up to 100−200 mg of MeAB and 2−3 mL of Al(BH$_4$)$_3$, and PXRD analysis confirms the synthesis of a single-phase sample of Al(BH$_4$)$_3$·MeAB (Figure 5).

Interaction of Al(BH$_4$)$_3$ with (CH$_2$NH$_2$BH$_3$)$_2$ and Formation of [Al(NH$_2$CH$_2$CH$_2$NH$_2$)(BH$_4$)$_2$][Al(BH$_4$)$_4$]. In order to study the interaction of Al(BH$_4$)$_3$ with EDBB, we used the same reaction procedure as that for the Al(BH$_4$)$_3$·NH$_3$BH$_3$ and Al(BH$_4$)$_3$·MeAB syntheses. In the reaction product, two types of crystal shapes were detected: flakes (major phase) and needles (minor phase). Structure determination on the needlelike crystals revealed the formation of [Al(en)(BH$_4$)$_2$][Al(BH$_4$)$_4$], suggesting the following reaction:

$$2Al(BH_4)_3 + (-CH_2NH_2BH_3-)_2$$

$$\rightarrow [Al(en)(BH_4)_2][Al(BH_4)_4] + B_2H_6 \quad (7)$$
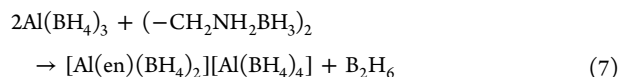
PXRD analysis of the sample reveals that the major phase is the starting EDBB, and either the fraction of [Al(en)(BH$_4$)$_2$][Al(BH$_4$)$_4$] is negligible or this complex is decomposing upon PXRD measurement.

Table 1 contains a summary on the products formed in the studied systems.

Table 1. Identified Products Forming in the Systems AlX$_3$−BH$_3$NH$_2$R [X = BH$_4^-$, Cl$^-$; R = −H, −CH$_3$, −(CH$_2$)$_2$NH$_2$BH$_3$]

component	Al(BH$_4$)$_3$	AlCl$_3$
NH$_3$BH$_3$	Al(BH$_4$)$_3$·NH$_3$BH$_3$[14]	NH$_4$AlCl$_4$, [NH$_3$BH$_2$NH$_3$]$^+$ (NMR)
MeAB (CH$_2$NH$_2$BH$_3$)$_2$	Al(BH$_4$)$_3$·MeAB [Al(en)(BH$_4$)$_2$] [Al(BH$_4$)$_4$]	[Al(MeAB)$_2$Cl$_2$][AlCl$_4$]

Single-Crystal X-ray Diffraction. Laboratory diffraction data for all of the measured single crystals were collected on a MAR345 image-plate detector (Mo Kα radiation; λ = 0.71073 Å; XENOCS focusing mirror). The crystals were loaded into inert grease in an Ar-filled glovebox and then measured at 150 K under a nitrogen flow (Oxford Cryosystems). The recorded data were indexed and integrated with *CrysAlisPRO*, and the implemented absorption correction was applied.[49] The structure of [Al(MeAB)$_2$Cl$_2$][AlCl$_4$] was solved in the orthorhombic space group *Pbca* with *a* = 12.5826(5) Å, *b* = 12.6510(5) Å, and *c* = 20.4039(8) Å. Al(BH$_4$)$_3$·MeAB crystallizes in the triclinic space group $P\bar{1}$ with *a* = 6.2764(3) Å, *b* = 7.9566(5) Å, *c* = 10.3058(8) Å, α = 70.28(1)°, β = 74.74(1)°, and γ = 86.04(1)°. [Al(NH$_2$CH$_2$CH$_2$NH$_2$)(BH$_4$)$_2$][Al(BH$_4$)$_4$] has a monoclinic structure, space group *P*2$_1$/*c* with *a* = 8.4168(5) Å, *b* = 12.0021(7) Å, *c* = 16.2933(12) Å, and β = 101.89(1)°.

All single-crystal data were solved by direct methods and refined by full-matrix least squares on F^2 using *SHELXL2014*.[50]

PXRD. The powders of the prepared MeAB and EDBB, as well as the products of their reactions with AlCl$_3$ and Al(BH$_4$)$_3$, were ground in an agate mortar inside an Ar-filled glovebox, and the powders were introduced into 0.7 mm glass capillaries and sealed with vacuum grease. Diffraction data were recorded on a MAR345 image-plate detector (Mo Kα radiation; λ = 0.71073; XENOCS focusing mirror). The obtained 2D images were azimuthally integrated by the program *Fit2D* using LaB$_6$ as the calibrant.[51]

Variable-temperature in situ synchrotron radiation PXRD on Al(BH$_4$)$_3$·MeAB and AlCl$_3$·AB samples was performed at the Materials Science Beamline (PSI in Villigen, Switzerland) using a Mython II detector (λ = 0.776190 Å). The capillaries were heated from 30 to 80 to 300 °C (ΔT/Δt = 5 °C/min), respectively.

TGA/DSC/MS Analysis. TGA and DSC analyses were made using a PerkinElmer STA 6000 apparatus simultaneously with MS analysis of the residual gas using a Hiden Analytical HPR-20 QMS sampling system. Samples (~5 mg) were loaded into Al crucibles and heated from room temperature to 200 °C (ΔT/Δt = 1 °C/min) in an argon flow of 40 mL/min. The released gas was analyzed in the ranges *m/z* 1−19, 21−39, and 41−50, omitting the characteristic *m/z* 20 and 40 for Ar.

Volumetric Study. Volumetric analysis was performed using a Hiden Isochema IMI-SHP analyzer. Decomposition experiments of the Al(BH$_4$)$_3$·MeAB complex were made with ~60 mg of sample, in 5 bar of back-pressure of H$_2$/He, and heated from 30 to 200 °C (ΔT/Δt = 1 °C/min). The gas release was calculated from the calibrated volumes of the system.

TPPA. The sample of Al(BH$_4$)$_3$·MeAB (~10 mg) was pressed into a pellet and sealed under an Ar atmosphere in a glass tube placed in a custom-made Al heating block.[52] The sample was heated from room temperature to 80 °C (ΔT/Δt = 1 °C/min). Photographs of the sample were collected every 1 min.

NMR Spectroscopy. All NMR spectra were recorded at room temperature (295 K) on a Bruker Avance 500 spectrometer operating at 500.13 MHz for ^{1}H, 160.46 MHz for ^{11}B, and 130.32 MHz for ^{27}Al. Experiments were run under the *TopSpin* program (1.3 version; Bruker) using a BBO{^{1}H,X} probehead equipped with a *z*-gradient coil. ^{1}H chemical shifts were referenced to the residual undeuterated C$_6$D$_6$ signal (7.16 ppm). ^{11}B and ^{27}Al NMR signals were referenced (δ = 0.00 ppm) according to the B and Al frequencies in the BF$_3$·Et$_2$O and Al(NO$_3$)$_3$ reference compounds. Standard zg programs were employed for 1D NMR experiments. An inverse-gated decoupling method with a Waltz-16 decoupling scheme using a pulse of 80 μs was used for ^{11}B{^{1}H} and ^{27}Al{^{1}H} NMR analyses.

■ ASSOCIATED CONTENT

ⓈSupporting Information

The Supporting Information is available free of charge on the ACS Publications website at DOI: 10.1021/acs.inorgchem.8b02630.

> Figures S1−S9 and Tables S1−S6 (PDF)
>
> NMR study data and spectra (PDF)

Accession Codes

CCDC 1871662−1871664 contain the supplementary crystallographic data for this paper. These data can be obtained free of charge via www.ccdc.cam.ac.uk/data_request/cif, or by emailing data_request@ccdc.cam.ac.uk, or by contacting The Cambridge Crystallographic Data Centre, 12 Union Road, Cambridge CB2 1EZ, UK; fax: +44 1223 336033.

■ AUTHOR INFORMATION

Corresponding Authors

*E-mail: iurii.dovgaliuk@esrf.fr.

*E-mail: yaroslav.filinchuk@uclouvain.be.

ORCID

Iurii Dovgaliuk: 0000-0003-1997-4748

Kasper T. Møller: 0000-0002-1970-6703

Torben R. Jensen: 0000-0002-4278-3221

Yaroslav Filinchuk: 0000-0002-6146-3696

Notes

The authors declare no competing financial interest.

■ REFERENCES

(1) Orimo, S.; Nakamori, Y.; Eliseo, J. R.; Züttel, A.; Jensen, C. M. Complex Hydrides for Hydrogen Storage. *Chem. Rev.* **2007**, *107*, 4111−4132.

(2) Ley, M. B.; Jepsen, L. H.; Lee, Y.-S.; Cho, Y. W.; Bellosta von Colbe, J. M.; Dornheim, M.; Rokni, M.; Jensen, J. O.; Sloth, M.; Filinchuk, Y.; Jørgensen, J. E.; Besenbacher, F.; Jensen, T. R. Complex Hydrides for Hydrogen Storage − New Perspectives. *Mater. Today* **2014**, *17*, 122−128.

(3) Chua, Y. S.; Chen, P.; Wu, G.; Xiong, Z. Development of Amidoboranes for Hydrogen Storage. *Chem. Commun.* **2011**, *47*, 5116−5129.

(4) Jepsen, L. H.; Ley, M. B.; Lee, Y.-S.; Cho, Y. W.; Dornheim, M.; Jensen, J. O.; Filinchuk, Y.; Jørgensen, J. E.; Besenbacher, F.; Jensen, T. R. Boron−Nitrogen Based Hydrides and Reactive Composites for Hydrogen Storage. *Mater. Today* **2014**, *17*, 129−135.

(5) Paskevicius, M.; Jepsen, L. H.; Schouwink, P.; Černý, R.; Ravnsbæk, D. B.; Filinchuk, Y.; Dornheim, M.; Besenbacher, F.; Jensen, T. R. Metal Borohydrides and Derivatives − Synthesis, Structure and Properties. *Chem. Soc. Rev.* **2017**, *46*, 1565−1634.

(6) Wolf, G.; Baumann, J.; Baitalow, F.; Hoffmann, F. P. Calorimetric Process Monitoring of Thermal Decomposition of B−N−H Compounds. *Thermochim. Acta* **2000**, *343*, 19−25.

(7) Baitalow, F.; Baumann, J.; Wolf, G.; Jaenicke-Rößler, K.; Leitner, G. Thermal Decomposition of B−N−H Compounds Investigated by Using Combined Thermoanalytical Methods. *Thermochim. Acta* **2002**, *391*, 159−168.

(8) Sutton, A. D.; Burrell, A. K.; Dixon, D. A.; Garner, E. B.; Gordon, J. C.; Nakagawa, T.; Ott, K. C.; Robinson, J. P.; Vasiliu, M. Regeneration of Ammonia Borane Spent Fuel by Direct Reaction with Hydrazine and Liquid Ammonia. *Science* **2011**, *331*, 1426−1429.

(9) Davis, B. L.; Rekken, B. D.; Michalczyk, R.; Garner, E. B., III; Dixon, D. A.; Kalviri, H.; Baker, R. T.; Thorn, D. L. Lewis Base Assisted B−H Bond Redistribution in Borazine and Polyborazine. *Chem. Commun.* **2013**, *49*, 9095−9097.

(10) Luo, J.; Wu, H.; Zhou, W.; Kang, X.; Fang, Z.; Wang, P. LiBH$_4$·NH$_3$BH$_3$: A New Lithium Borohydride Ammonia Borane Compound with a Novel Structure and Favorable Hydrogen Storage Properties. *Int. J. Hydrogen Energy* **2012**, *37*, 10750−10757.

(11) Wu, H.; Zhou, W.; Pinkerton, F. E.; Meyer, M. S.; Srinivas, G.; Yildirim, T.; Udovic, T. J.; Rush, J. J. A New Family of Metal Borohydride Ammonia Borane Complexes: Synthesis, Structures, and Hydrogen Storage Properties. *J. Mater. Chem.* **2010**, *20*, 6550−6556.

(12) Chen, X.; Yuan, F.; Gu, Q.; Yu, X. Synthesis, Structures and Hydrogen Storage Properties of Two New H-enriched Compounds: Mg(BH$_4$)$_2$(NH$_3$BH$_3$)$_2$ and Mg(BH$_4$)$_2$·(NH$_3$)$_2$(NH$_3$BH$_3$). *Dalton Trans.* **2013**, *42*, 14365−14368.

(13) Jepsen, L. H.; Ban, V.; Møller, K. T.; Lee, Y.-S.; Cho, Y. W.; Besenbacher, F.; Filinchuk, Y.; Skibsted, J.; Jensen, T. R. Synthesis, Crystal Structure, Thermal Decomposition, and ^{11}B MAS NMR Characterization of Mg(BH$_4$)$_2$(NH$_3$BH$_3$)$_2$. *J. Phys. Chem. C* **2014**, *118*, 12141−12153.

(14) Dovgaliuk, I.; Le Duff, C. S.; Robeyns, K.; Devillers, M.; Filinchuk, Y. Mild Dehydrogenation of Ammonia Borane Complexed with Aluminum Borohydride. *Chem. Mater.* **2015**, *27*, 768−777.

(15) Dovgaliuk, I.; Filinchuk, Y. Aluminium Complexes of B- and N-based Hydrides: Synthesis, Structures and Hydrogen Storage Properties. *Int. J. Hydrogen Energy* **2016**, *41*, 15489−15504.

(16) Summerscales, O. T.; Gordon, J. C. Regeneration of Ammonia Borane from Spent Fuel Materials. *Dalton Trans.* **2013**, *42*, 10075−10084.

(17) Bowden, M. E.; Brown, I. W. M.; Gainsford, G. J.; Wong, H. Structure and Thermal Decomposition of Methylamine Borane. *Inorg. Chim. Acta* **2008**, *361*, 2147−2153.

(18) Leardini, F.; Valero-Pedraza, M. J.; Perez-Mayoral, E.; Cantelli, R.; Bañares, M. A. Thermolytic Decomposition of Ethane 1,2-Diamineborane Investigated by Thermoanalytical Methods and in Situ Vibrational Spectroscopy. *J. Phys. Chem. C* **2014**, *118*, 17221−17230.

(19) Neiner, D.; Karkamkar, A.; Bowden, M.; Joon Choi, Y.; Luedtke, A.; Holladay, J.; Fisher, A.; Szymczak, N.; Autrey, T. Kinetic and Thermodynamic Investigation of Hydrogen Release from Ethane 1,2-di-amineborane. *Energy Environ. Sci.* **2011**, *4*, 4187−4193.

(20) Mairesse, G.; Barbier, P.; Wignacourt, J. P.; Rubbens, A.; Wallart, F. X-Ray, Raman, Infrared, and Nuclear Magnetic Resonance Studies of the Crystal Structure of Ammonium Tetrachloroaluminate, NH$_4$AlCl$_4$. *Can. J. Chem.* **1978**, *56*, 764−771.

(21) Chen, X.; Bao, X.; Zhao, J.-C.; Shore, S. G. Experimental and Computational Study of the Formation Mechanism of the Diammoniate of Diborane: The Role of Dihydrogen Bonds. *J. Am. Chem. Soc.* **2011**, *133*, 14172−14175.

(22) Zheng, X.; Huang, X.; Song, Y.; Ma, X.; Guo, Y. Aluminum Borohydride−Ethylenediamine as a Hydrogen Storage Candidate. *RSC Adv.* **2015**, *5*, 105618−105621.

(23) Gu, Q.; Wang, Z.; Filinchuk, Y.; Kimpton, J. A.; Brand, H. E. A.; Li, Q.; Yu, X. Aluminum Borohydride Complex with Ethylenediamine: Crystal Structure and Dehydrogenation Mechanism Studies. *J. Phys. Chem. C* **2016**, *120*, 10192−10198.

(24) Filinchuk, Y.; Černý, R.; Hagemann, H. Insight into Mg(BH$_4$)$_2$ with Synchrotron X-ray Diffraction: Structure Revision, Crystal Chemistry, and Anomalous Thermal Expansion. *Chem. Mater.* **2009**, *21*, 925−933.

(25) Filinchuk, Y.; Richter, B.; Jensen, T. R.; Dmitriev, V.; Chernyshov, D.; Hagemann, H. Porous and Dense Magnesium Borohydride Frameworks: Synthesis, Stability, and Reversible Absorption of Guest Species. *Angew. Chem., Int. Ed.* **2011**, *50*, 11162−11166.

(26) Bakhmutov, V. I. *Dihydrogen Bonds: Principles, Experiment, and Applications*; Wiley-Interscience: Hoboken, NJ, 2008.

(27) Groom, C. R.; Bruno, I. J.; Lightfoot, M. P.; Ward, S. C. The Cambridge Structural Database. *Acta Crystallogr., Sect. B: Struct. Sci., Cryst. Eng. Mater.* **2016**, *B72*, 171−179.

(28) Belsky, A.; Hellenbrandt, M.; Karen, V. L.; Luksch, P. New Developments in the Inorganic Crystal Structure Database (ICSD): Accessibility in Support of Materials Research and Design. *Acta Crystallogr., Sect. B: Struct. Sci.* **2002**, *B58*, 364−369.

(29) Del Grosso, A.; Ayuso Carrillo, J.; Ingleson, M. I. Regioselective Electrophilic Borylation of Haloarenes. *Chem. Commun.* **2015**, *51*, 2878−2881.

(30) Schick, G.; Loew, A.; Nieger, M.; Airola, K.; Niecke, E. Syntheses and Reactivity of Aminobis(diorganylamino)phosphanes. *Chem. Ber.* **1996**, *129*, 911−917.

(31) Dovgaliuk, I.; Ban, V.; Sadikin, Y.; Černý, R.; Aranda, L.; Casati, N.; Devillers, M.; Filinchuk, Y. The First Halide-Free Bimetallic Aluminum Borohydride: Synthesis, Structure, Stability, and Decomposition Pathway. *J. Phys. Chem. C* **2014**, *118*, 145−153.

(32) Dovgaliuk, I.; Safin, D. A.; Tumanov, N. A.; Morelle, F.; Moulai, A.; Łodziana, Z.; Černý, R.; Devillers, M.; Filinchuk, Y. Solid Aluminum Borohydrides for Prospective Hydrogen Storage. *ChemSusChem* **2017**, *10*, 4725−4734.

(33) Dou, D.; Liu, J.; Bauer, J. A. K.; Jordan, G. T., IV; Shore, S. G. Synthesis and Structure of Triphenylmethylphosphonium Tetrakis-(tetrahydroborato)Aluminate, [Ph₃MeP][Al(BH₄)₄], an Example of Eight-Coordinate Aluminum(III). *Inorg. Chem.* **1994**, *33*, 5443−5447.

(34) Lindemann, I.; Ferrer, R. D.; Dunsch, L.; Černý, R.; Hagemann, H.; D'Anna, V.; Filinchuk, Y.; Schultz, L.; Gutfleisch, O. Novel Sodium Aluminium Borohydride Containing the Complex Anion [Al(BH₄,Cl)₄]⁻. *Faraday Discuss.* **2011**, *151*, 231−242.

(35) Atwood, D. A. Cationic Group 13 Complexes. *Coord. Chem. Rev.* **1998**, *176*, 407−430.

(36) Aldridge, S.; Downs, A. J.; Tang, C. Y.; Parsons, S.; Clarke, M. C.; Johnstone, R. D. L.; Robertson, H. E.; Rankin, D. W. H.; Wann, D. A. Structures and Aggregation of the Methylamine−Borane Molecules, MeₙH₃₋ₙN·BH₃ (*n* = 1−3), Studied by X-ray Diffraction, Gas-Phase Electron Diffraction, and Quantum Chemical Calculations. *J. Am. Chem. Soc.* **2009**, *131*, 2231−2243.

(37) Grant, D. J.; Matus, M. H.; Anderson, K. D.; Camaioni, D. M.; Neufeldt, S. R.; Lane, C. F.; Dixon, D. A. Thermochemistry of Dehydrogenation of Methyl-Substituted Ammonia Borane Compounds. *J. Phys. Chem. A* **2009**, *113*, 6121−6132.

(38) Data from the *NIST Standard Reference Database 69: NIST Chemistry WebBook*; NIST, 2009.

(39) Borgschulte, A.; Callini, E.; Probst, B.; Jain, A.; Kato, S.; Friedrichs, O.; Remhof, A.; Bielmann, M.; Ramirez-Cuesta, A. J.; Züttel, A. Impurity Gas Analysis of the Decomposition of Complex Hydrides. *J. Phys. Chem. C* **2011**, *115*, 17220−17226.

(40) Lindemann, I.; Borgschulte, A.; Callini, E.; Züttel, A.; Schultz, L.; Gutfleisch, O. Insight Into the Decomposition Pathway of the Complex Hydride Al₃Li₄(BH₄)₁₃. *Int. J. Hydrogen Energy* **2013**, *38*, 2790−2795.

(41) Downs, A. J.; Jones, L. A. Hydridoaluminium Bis-(tetrahydroborate): A new Synthesis and Some Physical and Chemical Properties. *Polyhedron* **1994**, *13*, 2401−2415.

(42) Muhoro, C. N.; He, X.; Hartwig, J. F. Titanocene Borane σ-Complexes. *J. Am. Chem. Soc.* **1999**, *121*, 5033−5046.

(43) Sohail, M.; Moncho, S.; Brothers, E. N.; Darensbourg, D. J.; Bengali, A. A. Estimating the Strength of the M−H−B Interaction: a Kinetic Approach. *Dalton Trans.* **2013**, *42*, 6720−6723.

(44) Richardson, T.; de Gala, S.; Crabtree, R. H.; Siegbahn, P. E. M. Unconventional Hydrogen Bonds: Intermolecular B-H···H-N Interactions. *J. Am. Chem. Soc.* **1995**, *117*, 12875−12876.

(45) Karthikeyan, S.; Sedlak, R.; Hobza, P. on the Nature of Stabilization in Weak, Medium, and Strong Changre-Transfer Complexes: CCSD(T)/CBS and SAPT Calculations. *J. Phys. Chem. A* **2011**, *115*, 9422−9428.

(46) Fu, L.; Li, N.; Liu, Y.; Wang, W.; Zhu, Y.; Wu, Y. Advances of Aluminum Based Energy Storage Systems. *Chin. J. Chem.* **2017**, *35*, 13−20.

(47) Roedern, E.; Kühnel, R.-S.; Remhof, A.; Battaglia, C. Magnesium Ethylenediamine Borohydride as Solid-State Electrolyte for Magnesium Batteries. *Sci. Rep.* **2017**, *7*, 46189.

(48) Kelly, H. C.; Edwards, J. O. Evidence for the Open Chain Structure of Ethane 1,2-Diamineborane. *Inorg. Chem.* **1963**, *2*, 226−227.

(49) *Xcalibur/SuperNova CCD system, CrysAlisPro Software system*, version 1.171.36.24; Agilent Technologies U.K. Ltd.: Oxford, U.K., 2012.

(50) Sheldrick, G. M. A Short History of SHELX. *Acta Crystallogr., Sect. A: Found. Crystallogr.* **2008**, *A64*, 112−122.

(51) Hammersley, A. P.; Svensson, S. O.; Hanfland, M.; Fitch, A. N.; Häusermann, D. Two-Dimensional Detector Software: from Real Detector to Idealised Image or Two-Theta Scan. *High Pressure Res.* **1996**, *14*, 235−248.

(52) Paskevicius, M.; Ley, M. B.; Sheppard, D. A.; Jensen, T. R.; Buckley, C. E. Eutectic Melting in Metal Borohydrides. *Phys. Chem. Chem. Phys.* **2013**, *15*, 19774−19789.